STEM CELLS®

REGENERATIVE MEDICINE

Highly Purified Human Extracellular Vesicles Produced by Stem Cells Alleviate Aging Cellular Phenotypes of Senescent Human Cells

SENQUAN LIU,[a,b,*] VASILIKI MAHAIRAKI,[b,c,*] HAO BAI,[a,b] ZHENG DING,[a,b] JIAXIN LI,[b,c] KENNETH W. WITWER,[c,d] LINZHAO CHENG [a,b]

Key Words. Human induced pluripotent stem cells • Mesenchymal stem cells • Extracellular vesicles • Aging • Senescence • Peroxiredoxin

[a]Department of Medicine, Johns Hopkins University School of Medicine, Baltimore, Maryland, USA; [b]Institute for Cell Engineering, Johns Hopkins University School of Medicine, Baltimore, Maryland, USA; [c]Department of Neurology, Johns Hopkins University School of Medicine, Baltimore, Maryland, USA; [d]Department of Molecular and Comparative Pathobiology, Johns Hopkins University School of Medicine, Baltimore, Maryland, USA

*Contributed equally.

Correspondence: Linzhao Cheng, Ph.D., Johns Hopkins University School of Medicine, Miller Research Building 779, 733 North Broadway, Baltimore, Maryland 21205, USA. Telephone: 410-614-6958; e-mail: lcheng2@jhmi.edu; or Vasiliki Mahairaki, Ph.D., Johns Hopkins University School of Medicine, Miller Research Building, Room 775, 733 North Broadway, Baltimore, Maryland 21205, USA. Telephone: 410-258-0926; e-mail: vmachai1@jhmi.edu

Received November 19, 2018; accepted for publication February 17, 2019; first published online February 27, 2019.

http://dx.doi.org/10.1002/stem.2996

ABSTRACT

Extracellular vesicles (EVs), including exosomes and microvesicles, mediate intercellular communications and exert various biological activities via delivering unique cargos of functional molecules such as RNAs and proteins to recipient cells. Previous studies showed that EVs produced and secreted by human mesenchymal stem cells (MSCs) can substitute intact MSCs for tissue repair and regeneration. In this study, we examined properties and functions of EVs from human induced pluripotent stem cells (iPSCs) that can be cultured infinitely under a chemically defined medium free of any exogenous EVs. We collected and purified EVs secreted by human iPSCs and MSCs. Purified EVs produced by both stem cell types have similar sizes (~150 nm in diameter), but human iPSCs produced 16-fold more EVs than MSCs. When highly purified iPSC-EVs were applied in culture to senescent MSCs that have elevated reactive oxygen species (ROS), human iPSC-EVs reduced cellular ROS levels and alleviated aging phenotypes of senescent MSCs. Our discovery reveals that EVs from human stem cells can alleviate cellular aging in culture, at least in part by delivering intracellular peroxiredoxin antioxidant enzymes. STEM CELLS *2019;37:779–790*

SIGNIFICANCE STATEMENT

Recently, increasing evidence has supported the idea that mesenchymal stem cell (MSC)-derived extracellular vesicles (EVs) opened a new avenue for treating tissue injury. However, a major bottleneck in using MSC-derived EV-based applications in clinics is the inefficient production and purification of clinical-grade EVs. Surprisingly, recent results demonstrate that human induced pluripotent stem cells (iPSCs) produce great numbers of EVs under a defined culture condition, and the concentration is much higher than by MSCs. Furthermore, this study investigated the activities of iPSC-EVs and found that purified EVs from both stem cell types alleviate aging phenotypes of senescent MSCs. These EVs also alleviate progerin-induced senescence in premature aging cell model. Overall, the delivery of human iPSC-EVs attenuated cell aging and promoted cell proliferation, suggesting that highly purified EVs from human iPSCs may represent a cell-free approach for treating aging and degenerative diseases.

INTRODUCTION

Extracellular vesicles (EVs), including exosomes and microvesicles, are heterogeneous populations of naturally occurring nanosized vesicles released by almost all cell types [1]. They are enclosed by a lipid bilayer and range in size from a diameter from roughly 30 to 150 nm for endosomal system-derived exosomes and ~100–1,000 nm for cell surface-shed microvesicles [2]. EVs have emerged as novel and important players in intercellular communication, mainly through their ability to transfer biological content, consisting of proteins, lipids, and nucleic acids, to recipient cells [3, 4]. Recent research efforts have focused on leveraging EVs as a powerful therapeutic tool in tissue repair and regeneration [5–7]. Mesenchymal stem/stromal cells (MSCs) are one of the most commonly used cell types for classic cell therapy, as well as for potential EV-mediated therapies without using intact donor cells [8]. MSC-derived EVs have opened a new avenue for treating tissue injury in cardiovascular diseases [9], radiation damage to bone marrow hematopoietic cells [10], fracture healing [11], and neurodegeneration [12]. Despite these advances, a major bottleneck of MSC-derived EV (MSC-EV)-based applications in clinics is the inefficient production

and purification of clinical-grade EVs. Cultured MSCs, especially those derived from adult tissues, have a limited cell proliferation capacity even under rich culture conditions, that is, supplemented by fetal bovine serum (FBS) or human platelet lysates. However, FBS and platelet lysates also contain abundant EVs. Ongoing studies are evaluating the yields, functions, and EV production capacity of MSCs that are expanded with various defined media and other culture conditions [13, 14].

Unlike postnatal somatic cells, including MSCs, human induced pluripotent stem cells (iPSCs) can be expanded in culture indefinitely while maintaining full developmental potential. In the past several years, completely defined culture medium was developed to expand human iPSCs on standard cell culture vessels coated with recombinant human vitronectin proteins [15]. We and others have shown evidence that the Essential 8 (E8) media system maintains the pluripotency and genomic stability of human iPSCs after extensive culture [15, 16]. With this recent breakthrough, it is no longer a major hurdle to expand human iPSCs efficiently under clinically compliant culture conditions. This highly defined and efficient iPSC culture system also makes it much easier to analyze numbers and functions of EVs made by human iPSCs [17]. However, very few studies describe the properties and functions of human iPSC-derived EVs [13, 18, 19], as compared with dozens of papers on MSC-EVs [8]. Additionally, most published applications of EVs used EVs from iPSC-derived committed cell types such as MSCs and cardiomyocytes instead of EVs from iPSCs [20–23]. However, the EV preparations (mainly by concentration using ultracentrifugation and polymer-mediated precipitation) in these previous studies were relatively impure, containing undefined soluble and aggregated proteins [24, 25].

In this study, we examined physical properties and biological functions of iPSC-EVs in comparison with MSC-EVs. Following international standards for EV characterization and purification [24, 25], we obtained highly purified EVs from both cell types, although many more were produced by human iPSCs. Using two different cellular senescence models, we observed that highly purified iPSC-EVs and MSC-EVs alleviated cellular senescence and promoted cell growth. Our results suggest that purified EVs from human stem cells may represent a cell-free approach for attenuating aging and treating degenerative diseases.

Materials and Methods

Cell Culture and EV Collection

Human iPSCs were maintained in Essential 8 medium on a vitronectin coated dish (all from Gibco, Carlsbad, CA) [26]. The medium was changed daily and cells were passaged at 80%–90% confluence using TrypLE Express Enzyme (Gibco) supplemented with 10 μM Y-27632 (Stem Cell Technologies, Vancouver, Canada). Cells used for EV collection were between passages 30 and 50 for EV collection. We presented the data of EV production using six different iPSC lines derived from diverse types of somatic cells of both genders (Supporting Information Table S1). Two iPSC lines were used extensively throughout the whole study including analyzing their biological functions: (a) BC1 reprogrammed from blood cells of a healthy male donor [27]; and (b) WT4 reprogrammed from fibroblasts of a healthy female donor [28]. We also used four different MSC preparations derived from three genetically distinct donors (Supporting Information Table S1). All MSCs were expanded with a standard MSC culture medium [29]: 90% Dulbecco's modified Eagle's medium with low glucose (Gibco), 10% FBS and other supplements. Two sources of adult MSCs were used throughout the whole study including analyzing biological functions of EVs derived from them: (a) MSCs derived from adult marrow of the same donor as for the established BC1 iPSCs; and (b) established MSCs from marrow of another adult healthy donor, obtained from Lonza (Cat #PT-2501 and Lot #0000654251). After MSCs reached ~70% confluence under the standard culture condition, we washed the cells with phosphate-buffered saline (PBS) and cultured them in E8 medium. We collected MSC-EVs daily in the next 3–5 days. Established human umbilical vascular endothelial cells (HUVECs) were bought from Lonza and cultured in the recommended EGM2 medium. Cultured cells were regularly tested to ensure they lack mycoplasma contamination.

EV Purification

Conditioned media were centrifuged at 300*g* for 10 minutes followed by 2,000*g* for 10 minutes at 4°C to remove cells and cellular debris. Amicon Ultra-15 Centrifugal Filters (Ultracel—100 K; Merck Millipore, Billerica, MA) were then used to concentrate EVs and filter out small proteins. Size exclusion chromatography (SEC) using qEV columns (Izon Science, Cambridge, MA) was performed with the filtration retentate for further purification of EVs. Briefly, after rinsing the qEV columns with PBS, 0.5 ml of concentrated EVs were applied to the top of the columns. Eluate was collected in sequential fractions of 0.5 ml according to the manufacturer's instructions. Eluted fractions enriched with EVs (8–10) were pooled and either analyzed directly or used for cell-based assays.

EV Measurement

Size distribution and concentration measurement were conducted on a second generation nanoparticle tracking analysis (NTA) instrument, the ZetaView (Particle Metrix, Germany) with a 488-nm laser and software ZetaView 8.04.02. Temperature was controlled at 24°C. The data acquisition parameters were set as follows: positions (11), cycles number (1), sensitivity (85), frame rate (30), shutter (70), minimum brightness (20), max size (1,000), and min size (5). All parameters were recommended by the manufacturer for EV analysis. After initial wash and calibration, samples were diluted to $3 \times 10^7 \sim 1 \times 10^8$ particles per milliliter in PBS.

Transmission Electron Microscopy

Purified EVs were covered with Formvar-carbon-coated EM grids to promote the absorption of EVs onto membranes over 20 minutes in a dry environment at room temperature. The grids were then placed directly on a drop of 1% glutaraldehyde and incubated for 5 minutes to remove the negative background. The grids were washed seven times with distilled water for 2 minutes each and examined using a Philips/FEI BioTwin CM120 Transmission Electron Microscope at an acceleration voltage of 120 kV using a Gatan Orius high-resolution cooled digital camera.

EV Labeling and Uptake by Cells

Purified EVs were stained with 10^{-6} M PKH26 or PKH67 Cell Membrane Labeling Dye (Sigma–Aldrich, St. Louis, MO) according to the manufacturer's instructions. Excess dye was removed using exosome spin columns (MW 3000; ThermoFisher Scientific, Carlsbad, CA) per the manufacturer's instructions. Labeled EVs were added to the recipient cells (10^5 EVs per cells) and incubated for 24 hours. After treatment, cells were washed twice with PBS and changed to fresh medium. Fluorescence intensity

was measured with a Celigo high-throughput micro-well image cytometer (Nexcelom Bioscience, Lawrence, MA) using its analysis program. The parameters of data acquisition and analysis were set as follows: intensity threshold (4), precision (high), cell diameter (20), dilation radius (0 pixel), cell intensity range (0–255), and cell area (10–10,000 in setting).

Cell Growth Assays Using AlamarBlue Florescent Dye

After treatment of cells with EVs, 10 μl of AlamarBlue reagent (ThermoFisher Scientific) was added to each well. Cells were incubated for 1 hour in an incubator at 37°C, 5% CO_2. Fluorescence intensity was measured with excitation at 550 nm and emission at 590 nm on a Celigo high-throughput micro-well image cytometer (Nexcelom Bioscience).

Establishment of a Progerin-Induced Senescence Model

To establish a progerin-induced senescence cell model, progerin vector (Addgene plasmid 22662, Cambridge, MA) was used to produce lentivirus then transduce normal human MSCs (at early-passages and proliferating). Briefly, the progerin construct (pCDH-CMV-progerin-EF1a-balstcidin vector) or green fluorescent protein (GFP)-expressing control construct pCDH-CMV-GFP (modified from Addgene plasmid 72265) was co-transfected with two packaging plasmids pMD2.G (Addgene plasmid 12259) and psPAX2 (Addgene plasmid 12260) on 293 T cells using Lipofectamine 2000 (ThermoFisher Scientific). Lentiviral particles were concentrated using an Amicon concentration column (with a membrane of 100 kDa cutoff, Sigma-Millipore). We did not further enrich progerin transduced MSCs because the transduction efficiency is estimated to be >95% (either by flow cytometry analysis or immunostaining of individual cells).

WST-1 Colorimetric Assay for Measuring Cell Growth

Proliferation was measured with water-soluble tetrazolium salt (WST-1) reagent according to manufacturer instructions (Merck Millipore). Briefly, cells were cultured in a 96-well plate in a final volume of 100 μl per well culture medium in the absence or presence of purified EVs. After treatment, 10 μl per well WST-1 solution was added to each well, and cells were incubated for 4 hours in standard culture conditions. Absorbance at 450 nm was measured in triplicate wells using a microplate reader (Bio-Rad, Hercules, CA).

EdU Assay to Measure DNA Synthesis

A cell proliferation assay based on DNA synthesis was performed with Click-iT Plus EdU Alexa FluorTM 488 Imaging Kits (ThermoFisher Scientific) according to the manufacturer's instruction. Briefly, cells were incubated with 10 μM EdU solution for 4 hours at 37°C. Cells were fixed in 3.7% formaldehyde in PBS for 15 minutes and permeabilized with 0.5% Triton X-100 for 20 minutes. Afterward, freshly prepared reaction cocktail was added, and cells were incubated at room temperature away from light for 30 minutes. Lastly, cellular DNA was stained with 5 μg/ml Hoechst 33342 or DAPI (4′,6-diamidino-2-phenylindole, dihydrochloride) solution and incubated for 30 minutes at RT in the dark. Washing steps were performed with PBS except during fixation and permeabilization steps, when 3% bovine serum albumin (BSA) in PBS was used. Proliferation index was then determined by quantifying the fraction of EdU-labeled cells/DNA-dye-labeled cells using a Celigo High Throughput Micro-Well Image Cytometer (Nexcelom Bioscience).

SA-β-Gal Staining for Senescent Cells

SA-β-Gal staining was performed as described previously [17] using a Senescence β-Galactosidase Staining Kit (Cell Signaling Technology, Danvers, MA). Briefly, cultured cells were washed in PBS and fixed at room temperature for 15 minutes with 4% formaldehyde in PBS. Fixed cells were stained with the SA-β-Gal staining solution and then incubated overnight at 37°C. Percentages of SA-β-Gal positive cells were then calculated.

Apoptosis Analysis

For cell apoptosis analysis, cells were collected and stained with Dead Cell Apoptosis Kit with Annexin V conjugated with the Alexa Fluor 488 dye and propidium iodide (both are from ThermoFisher Scientific). Apoptotic cells were analyzed using a BD FACSCalibur fluorescence assisted cell sorting (FACS) machine (BD Biosciences, San Diego, CA). Data analysis was performed with FlowJo software (FlowJo, Ashland, OR).

Enzyme-Linked Immunosorbent Assay for Detecting Secreted Cytokines

Enzyme-linked immunosorbent assay MEH-004A Multi-Analyte ELISArray Kit (Qiagen, Hilden, Germany) was used to measure the levels of cytokines and chemokines according to the manufacturer's instructions. Briefly, after preparing the reagents, assay buffer and samples were added continuously into each well of the provided plate. For positive and negative controls, antigen standards and sample dilution buffer were used, respectively. The plate was incubated for 2 hours at room temperature before washing and adding detection antibody. Another incubation for 1 hour at room temperature allowed the antibody to bind its specific proteins. After incubation, the unbound proteins were washed and biotinylated detection antibody Advin-HRP was added for 30 minutes in the dark. Substrate development solution was added after quadruple washing. After 15 minutes of incubation, the solution expressed blue color in proportion to the amount of protein analyte in the initial sample. Finally, stop solution was added to halt the development, enabling absorbance reading of the plate. The plate was processed by iMark Microplate Absorbance Reader (Bio-Rad). The corrected absorbance values were obtained by subtracting the absorbance at 570 nm from the absorbance at 450 nm. Protein levels were determined using the corresponding standard curve.

Quantitative PCR for Detecting mRNA Expression Levels

Total RNA was extracted using Quick-RNA MiniPrep Kit (Zymo Research, Orange, CA) according to the manufacturer's instructions. Reverse transcription was accomplished with 0.45 μg of total RNA using random primers and SuperScript III First-Strand Synthesis Kit for reverse transcription polymerase chain reaction (RT-PCR) (ThermoFisher Scientific). qPCR assays were performed in duplicate on a StepOnePlus PCR machine (Applied Biosystems) using SYBR Green PCR Master Mix (Applied Biosystems). Primers were synthesized by Sigma–Aldrich. For each sample, differences in threshold cycle values (ΔCt) were calculated by adjusting the Ct of the gene of interest to the Ct of the reference gene GAPDH.

Primers used were as follows: *p21* F (5′-GACACCACTGGAGGG TGACT-3′) and *p21* R (5′-CAGGTCCACATGGTCTTCCT-3′), *p53* F (5′-GCCCAACAACACCAGCTCCT-3′) and *p53* R (5′-CCTGGGCATCCTT

GAGTTCC-3′), *GAPDH* F (5′-CAATGACCCCTTCATTGACC-3′) and *GAPDH* R (5′-GACAAGCTTCCCGTTCTCAG-3′).

Western Blotting

Human iPSCs, MSCs and purified EVs were lysed in RIPA Buffer (ThermoFisher Scientific) supplemented with protease and phosphatase inhibitor cocktails (Roche, Nutley, NJ), followed by centrifugation at 16,000 *g* for 20 minutes at 4°C. Protein quantification of cell and EV lysates was conducted using a Pierce BCA Protein Assay Kit (ThermoFisher Scientific). Lysates were resolved using a 4%–12% NuPage gel, then transferred onto nitrocellulose membrane (GE Healthcare, California, USA). Blots were probed using primary antibodies in 1× TBST (Tris-buffered Saline containing 0.1% Tween-20% and 5% Blotting grade blocker) purchased from Bio-Rad. Primary antibodies used included anti-CD81 (Santa Cruz, Cat #SC166029, Dallas, TX), anti-Calnexin (Abcam, Cat #ab22595, Cambridge, MA), anti-TSG101 (Abcam, Cat #ab125011), anti-Syntenin (Abcam, Cat #ab133267), anti-PRDX1 (ThermoFisher Scientific, Cat #LF-MA0073), anti-PRDX2 (ThermoFisher Scientific, Cat #LF-MA0144), and anti-GAPDH (Cell Signaling Technology, Cat #5174). Secondary antibodies used included goat anti-mouse IgG (H + L; LI-COR Biosciences, Cat #P/N 925–32,210, Lincoln, NE) and goat anti-rabbit IgG (H + L; LI-COR Biosciences, Cat #P/N 925–32,211).

Reactive Oxygen Species Detection

To measure oxidative stress levels, CellROX Green reagent (ThermoFisher Scientific) was added into human MSCs at a final concentration of 500 nM in complete growth medium and incubated for 60 minutes at 37°C, protected from light. Stained samples were collected and analyzed using a BD FACSCalibur FACS machine (BD Biosciences). Data analyses were performed with FlowJo software (FlowJo).

γ-H2AX Staining to Measure DNA Damage Levels

The levels of γ-H2AX in chromosomal DNA, as a hallmark of DNA damages in senescent cells, were performed according to manufacturer instructions (Merck Millipore). Briefly, cells with or without treatment or senescence were fixed in 4% formaldehyde for 10 minutes, permeabilized with 0.2% Triton X-100 in PBS for 10 minutes, and blocked with 5% FBS for 2 hours. Then the treated cells were incubated overnight at 4°C with γ-H2AX primary antibody (Merck Millipore Cat #05-636), diluted 1:250 in blocking buffer. On the next day, cells were washed with PBS twice and incubated for 1 hour with secondary antibodies (Alexa Fluor goat-anti-mouse 488, ThermoFisher Scientific, Cat #A11029, 1:500 dilution) together with 5 μg/ml DAPI. Fluorescence intensities of γ-H2AX and DNA staining were measured with a Celigo high-throughput micro-well image cytometer (Nexcelom Bioscience).

Proteomics and Gene Ontology Analysis

Protein samples were solubilized in urea and Tris, reduced with DTT, and alkylated with iodoacetamide at room temperature, protected from light. Then proteolysis with trypsin was performed for 3 hours, and the resulting peptides were desalted. Liquid chromatography–mass spectrometry (LC-MS)/MS analysis of digested peptides was performed on an Orbitrap Q Exactive Plus mass spectrometer. Data were managed using MaxQuant against a human database. Quantification of the identified proteins was performed using the Intensity Based Absolute Quantification (iBAQ) algorithm in MaxQuant. Protein IDs in samples that were either not associated with a protein name or showed 0 by iBAQ analysis were excluded from analysis. Common proteins were compiled with MATLAB R2018a. Gene ontology on common genes was performed with FunRich 3.1.3 (http://www.funrich.org/). FunRich database was used for Bonferroni correction to *p*-values. Venn diagram is drawn by Venn Diagram Plotter.

Statistical Analysis

Statistical testing was performed with GraphPad Prism 7.0 software. A two-tailed Student's *t* test was performed for two-group comparisons, or one-way analysis of variance for comparisons involving three or more groups. *p* values <.05 were considered significant, as indicated by * or otherwise indicated in figure legends. All cell culture data shown in the article are representative of experiments conducted at least three times.

Results

Production of Biological Nanoparticles From Human iPSCs and MSCs Collected in Cell Culture Supernatants Under a Chemically Defined Culture Condition

Human iPSCs were expanded using recombinant human vitronectin as an adherent substrate and the chemically defined E8 medium, refreshed daily. After cells reached ∼70% confluence, conditioned medium was collected daily for 3–5 days. We used a second generation NTA instrument, ZetaView, to measure the concentration of EVs produced by multiple human iPSC lines, which were reprogrammed from different donors and from human peripheral blood mononuclear cells or MSCs/fibroblasts [27, 28, 30]. The mean hydrodynamic diameter of these nanoparticles as a single peak was ∼150 nm (Fig. 1A, 1B). We extensively analyzed the EV production from six iPSC lines derived from diverse somatic cell types and genetic background (Supporting Information Fig. S1A, S1B). On average of 16 unique biological samples measured, nanoparticle concentrations were on average 7.5×10^9 per milliliter from multiple human iPSCs lines (Fig. 1C).

We also attempted to measure EVs produced by human MSCs in culture. To overcome the hurdle that FBS also contains abundant exogenous EVs, we collected MSC-produced EVs in the same E8 medium used for iPSC culture, which is free of exogenous EVs (Supporting Information Fig. S1C). After MSCs reached ∼70% confluence under the standard culture condition, we washed the cells with PBS and cultured them in E8 medium. We collected MSC-EVs daily in the next 3–5 days. MSCs cultured in E8 medium remained viable for at least 7 days, with minimal numbers of apoptotic cells examined on day 5 (Supporting Information Fig. S1D). EVs produced by MSCs had a mean diameter of ∼150 nm (different from ∼100 nm EVs in FBS or exosome-depleted FBS; Supporting Information Fig. S1E, S1F). Using multiple MSC cultures at early passages (p2–p6), we observed that the concentration of adult MSC-derived nanoparticles was approximately 4.5×10^8 per milliliter (Fig. 1C; Supporting Information Fig. S1G). This is >16-fold lower than iPSC-EVs collected in the same medium. We also examined the concentration of EVs produced by other two types of human MSCs: umbilical cord-derived MSCs and MSCs differentiated from BC1 iPSCs (BC1-MSCs; Supporting Information Fig. S1A, S1B). Combining these data, we conclude that human iPSCs produced

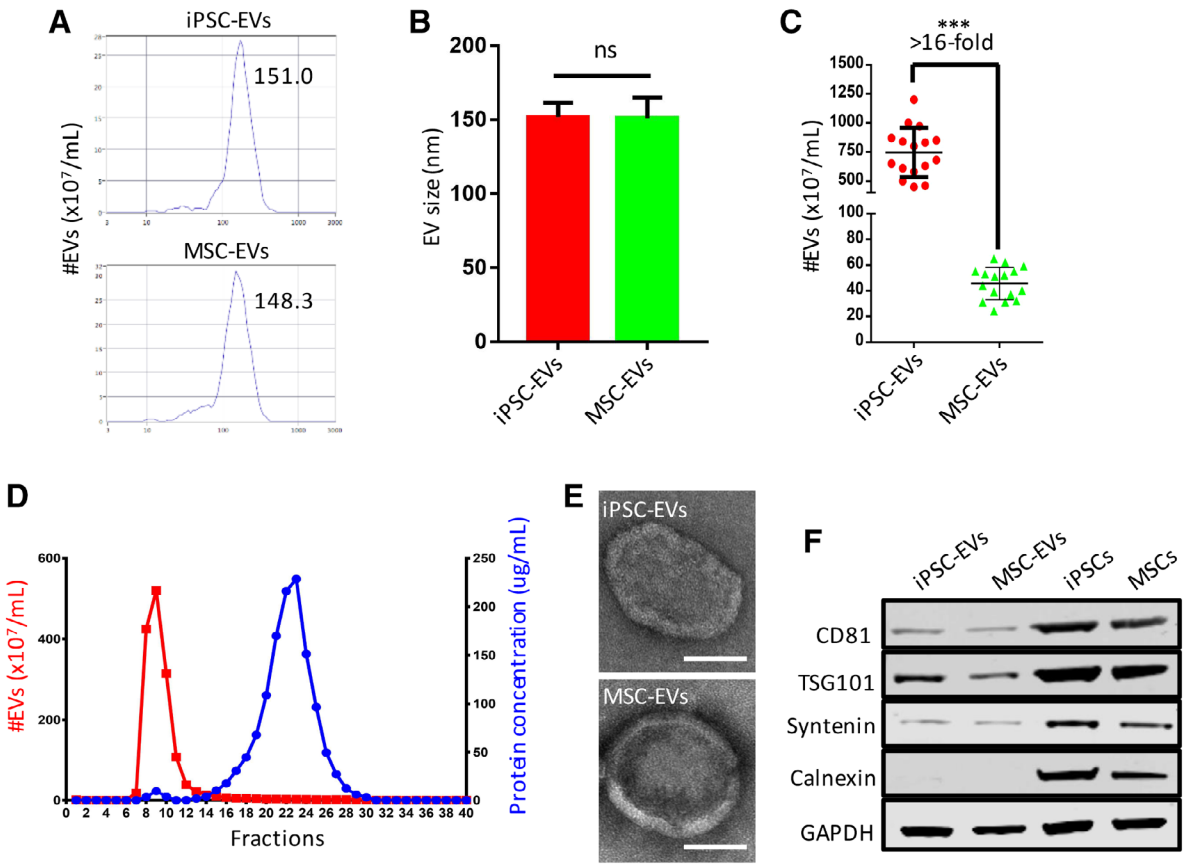

Figure 1. Production and purification of extracellular vesicles (EVs) secreted by human induced pluripotent stem cells (iPSCs) and mesenchymal stem cells (MSCs) cultured with a chemically defined medium. **(A):** Nanoparticle tracking analysis measurements of sizes and concentrations of EVs produced by human iPSCs and MSCs after an optimal dilution of 1:200 and 1:20 in volume, respectively. **(B):** Sizes of iPSC-EVs and MSC-EVs of multiple cultures (n = 16). **(C):** Concentrations of undiluted iPSC-EVs and MSC-EVs of multiple cell lines or cultures (n = 16). **(D):** Purification of concentrated iPSC-EVs by qEV size exclusion chromatography. **(E):** Representative images of iPSC-EVs and MSC-EVs by transmission electron microscopy. Scale bar: 100 nm. **(F):** Western blots to examine the presence or absence of indicated proteins in lysates of EVs or their producing cells. All data reflect mean ± SD from ≥3 independent experiments. Abbreviation: ns, not significant; ***, $p < .001$. Also see Supporting Information Figure S1.

EVs ~16-fold more efficiently than various types of MSCs in culture by using a chemically defined medium.

Purification and Characterization of EVs Produced by Human iPSCs and MSCs

To purify EVs from protein aggregates and other contaminants, the conditioned medium of iPSC and MSC cultures was concentrated using a filter with 100 kDa molecular weight cutoff, followed by SEC (qEV columns) of the retentate. EVs were eluted from SEC columns mainly in three peak fractions, whereas the majority of proteins were eluted thereafter. We estimated purity by comparing particle counts and total protein concentration across different fractions. Shown in Figure 1D, EVs were highly enriched and separated from other proteins in the conditioned medium of cultured iPSCs. We also applied the same purification scheme to MSC-EVs, although the EV concentration after purification from MSC samples was also ~16-fold lower than that from iPSC-EVs (data not shown). NTA measurements of purified iPSC-EVs and MSC-EVs showed a tighter peak of comparable size (~150 nm), confirmed by transmission electron microscopy that also displays typical EV morphology (Fig. 1E). Expression of specific proteins was assessed in purified EVs and cell lysates by Western Blot (Fig. 1F), confirming the presence of EV-associated proteins like CD81, TSG101, and syntenin, but the absence of calnexin, a calcium-binding, ER-associated protein.

Highly Purified iPSC-EVs Enter Target Cells More Efficiently than MSC-EVs

We next examined the uptake of iPSC-EVs by human MSCs and endothelial cells such as HUVECs. Purified EVs from iPSCs and MSCs in equal numbers were labeled with either PKH67 or PKH26 dyes, which emit green or red fluorescence, respectively, and integrate into lipid bilayer membranes. After removal of free dyes, we confirmed that membrane-labeling efficiencies were similar (Supporting Information Fig. S2E). After 24 hours of incubation with equal numbers of EVs, labeled EVs were readily found inside cells (mainly in perinuclear regions) as examined by fluorescence microscopy or scanner cytometry (Fig. 2). EVs labeled with either PKH67 or PKH26 could efficiently enter MSCs as well as HUVECs. Internalization efficiency of iPSC-EVs was higher than that of MSC-EVs. A time course analysis (Fig. 2G; Supporting Information Fig. S2A) further confirmed that EVs produced by iPSCs were more efficiently uptaken than those produced by MSCs. In addition, the results of EV internalization

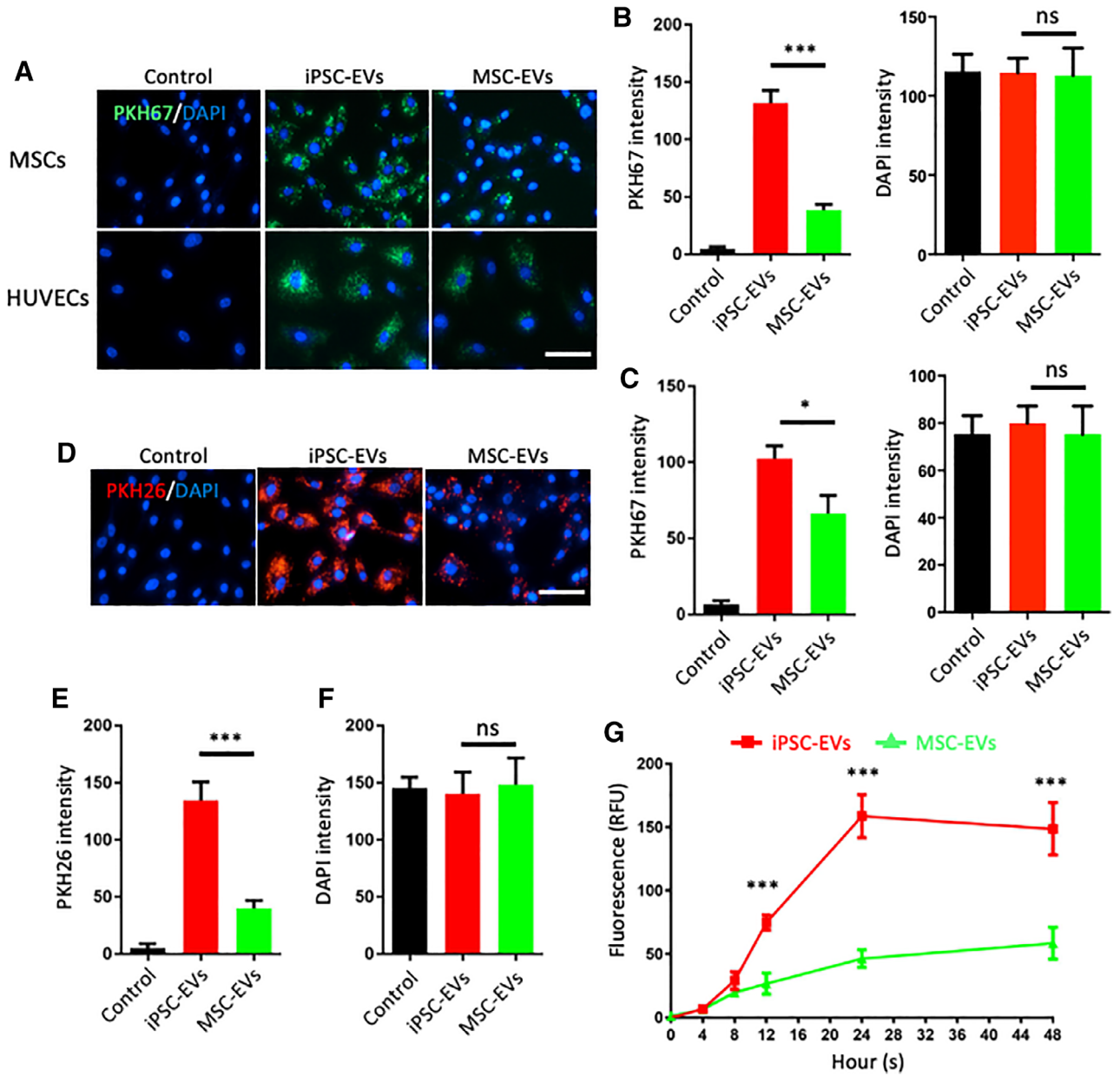

Figure 2. Highly purified extracellular vesicles (EVs) from human induced pluripotent stem cells (iPSCs) enter target cells efficiently. **(A):** Representative images of iPSC-EV and mesenchymal stem cell (MSC)-EV uptake by MSCs (upper) and human umbilical vascular endothelial cells (HUVECs; lower) after PKH67 green fluorescent dye labeling. Scale bar: 50 μm. **(B, C):** Quantification of PKH67 staining intensity in MSCs **(B)** and HUVECs **(C)**. **(D):** Representative images of iPSC-EV and MSC-EV uptake by MSCs after PKH26 red fluorescent dye labeling. Scale bar: 50 μm. **(E, F):** Quantification of PKH26 staining (E) and DAPI (4′,6-diamidino-2-phenylindole,dihydrochloride) staining (F) intensity in MSCs. **(G):** Time-course analysis of iPSC-EV and MSC-EV uptake by MSCs after PKH26 red fluorescent dye labeling of EVs. All data reflect mean ± SD from three independent experiments. Abbreviation: ns, not significant; *, $p < .05$; ***, $p < .001$. Also see Supporting Information Figure S2.

from BC1 iPSCs and the isogenic iPSC-derived MSCs further support our conclusion (Supporting Information Fig. S2B–S2D).

Human Stem Cell-Derived EVs Improve the Growth of Replicatively Aged MSCs

We next explored if highly purified EVs could alter biological functions of target cells in culture. We first incubated either iPSC-EVs or MSC-EVs with recipient cells that were actively proliferating at early passages (Supporting Information Fig. S2F, S2G). At a dose of 10,000 EVs per cell, we saw little effect on the growth of these proliferative MSCs and HUVECs compared with a PBS control. However, when senescent, serially passaged MSCs (>p10) were used [30], we observed that purified EVs from both cell types stimulated the growth of the otherwise senescent MSCs as measured by AlamarBlue-based assay (Fig. 3A). Similar growth enhancement was observed in a different cell-based assay using the WST-1 dye (Supporting Information Fig. S3A, S3B).

We next examined the effects of EVs on cell proliferation or apoptosis of senescent MSCs. After EV treatment for 4 days, the nucleotide analog EdU was added to the medium (Fig. 3B).

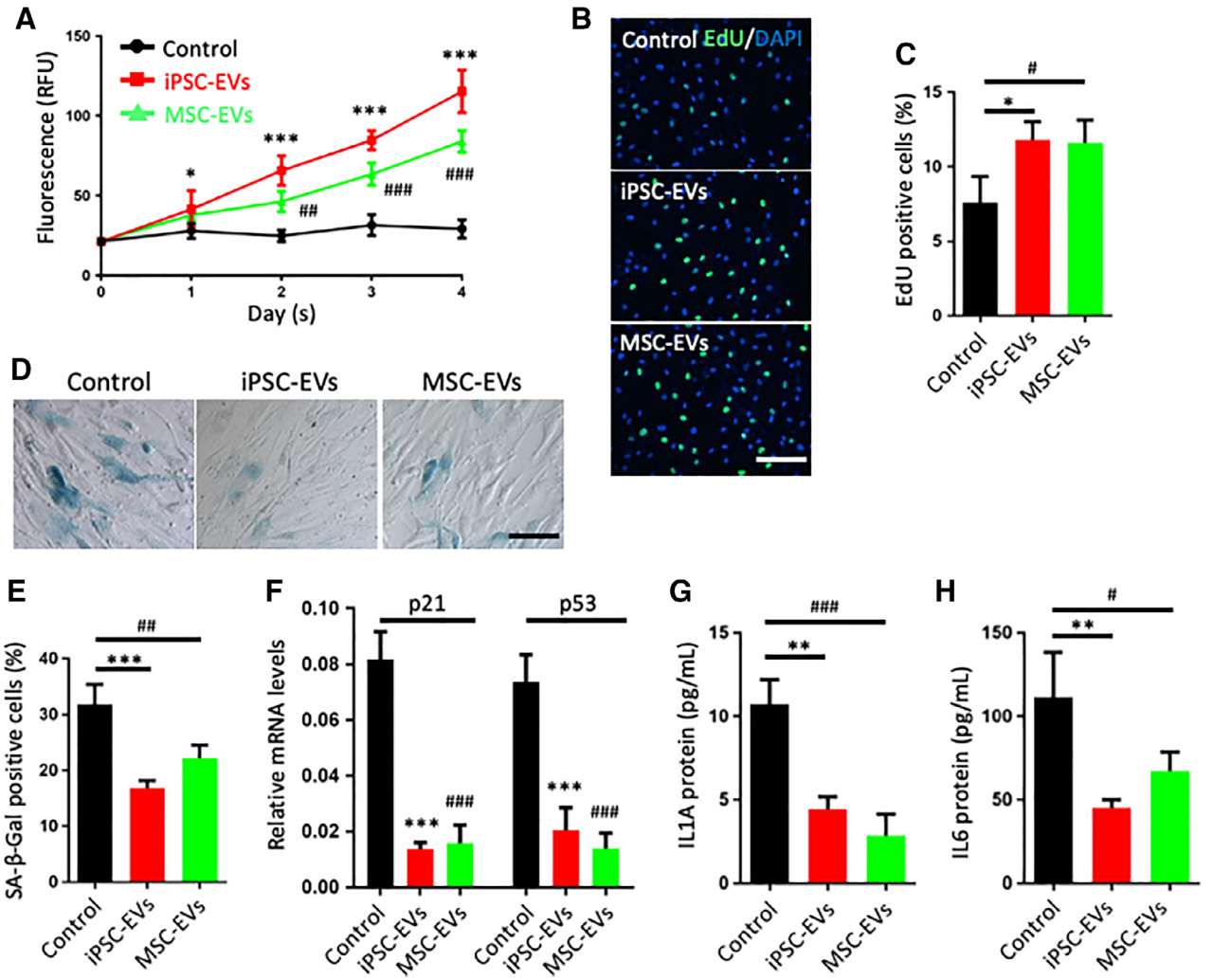

Figure 3. Human stem cell-derived extracellular vesicles (EVs) improve the growth of replicatively senescent mesenchymal stem cells (MSCs). **(A):** AlamarBlue assay to assess the cell growth of culture-aged MSCs (in passages of 10–14) incubated with induced pluripotent stem cell (iPSC)-EVs or MSC-EVs. **(B):** Representative images of iPSC-EV- or MSC-EV-treated MSCs incubated with EdU nucleotide analog. Scale bar: 100 μm. **(C):** Percentages of EdU positive cells after EV treatment of replicatively aged MSCs. **(D):** Representative images of SA β-gal staining for aged MSCs in the presence or absence of EVs. Scale bar: 50 μm. **(E):** Percentage of SA-β-gal positive aged MSCs after EV treatment. **(F):** Real-time qPCR to detect *p21* and *p53* gene expression after iPSC-EV and MSC-EV treatment. Human GAPDH was used as internal control. **(G):** Levels of senescence-associated secretory proteins interleukin (IL)-1a, measured by enzyme-linked immunosorbent assay (ELISA). **(H):** Levels of senescence-associated secretory proteins IL-6, measured by ELISA. All data reflect mean ± SD from four independent experiments. *, $p < .05$; **, $p < .01$; ***, $p < .001$; #, $p < .05$; ##, $p < .01$; ###, $p < .001$. Also see Supporting Information Figure S3.

The numbers of treated cells that incorporated EdU into nuclei significantly increased after EV treatments (Fig. 3C). However, there was little difference in the percentage of apoptotic cells (Supporting Information Fig. S3E, S3F). We also measured aging phenotypes of senescent MSCs after EV treatment, using well established assays [31]. We observed alleviation of aging phenotypes after EV treatment, such as reduction of cells expressing senescence-associated β-gal enzymatic activity (Fig. 3D, 3E), reduced expression of genes such as *p21* and *p53* (Fig. 3F), and reduced production of cytokines such as IL-1a and IL-6 (Fig. 3G, 3H). The increased production and secretion of cytokines such as IL-6 is a hallmark of the senescence-associated secretory phenotype (SASP). We also performed staining of senescent MSCs to examine the level of the γ-H2AX protein, another hallmark of cellular senescence and increased DNA damage. We found human stem cell-derived EVs also reduced the level of the γ-H2AX protein (Supporting Information Fig. S3C, S3D). Although EVs from both types of human stem cells could alleviate the senescent phenotypes of replicatively aged MSCs, iPSC-EVs consistently showed a modest improvement over MSC-EVs in enhancing cell growth (Fig. 3A; Supporting Information Fig. S3B), in addition to the fact that they are more abundantly produced by iPSCs in culture.

Human Stem Cell-Derived EVs Also Alleviate Cellular Aging in a Genetically Induced Senescence Model

In addition to the senescent MSCs after serial and exhausting passaging as a replicative aging model, we also used a premature aging model of cellular senescence. Replicative, early-passage MSCs (p3–p6) were transduced with progerin, a mutant form of the nuclear architectural protein lamin A [32]. Production of progerin in connective tissues causes Hutchinson–Gilford Progeria

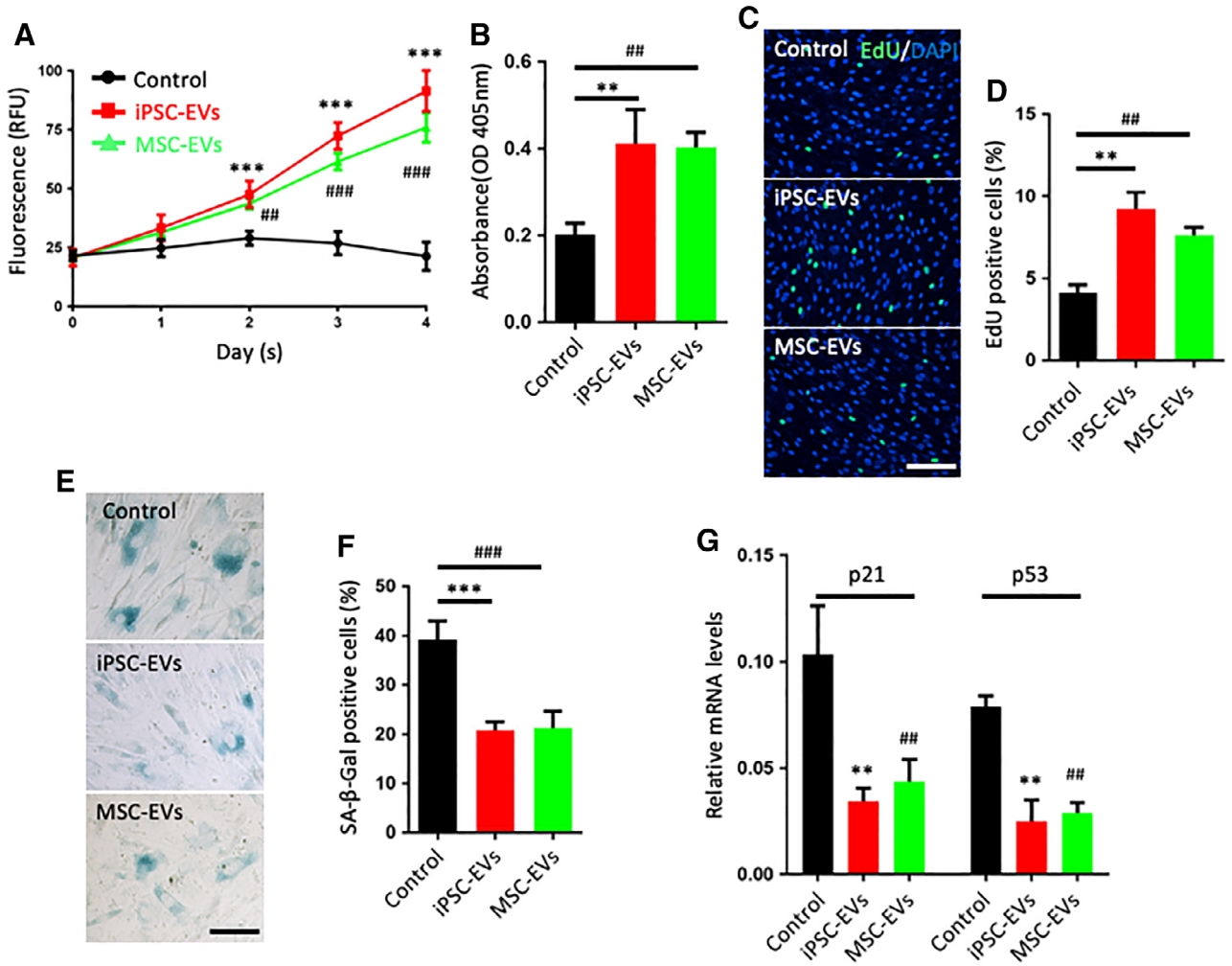

Figure 4. Human stem cell-derived extracellular vesicles (EVs) alleviate cellular aging in a genetically induced senescence model. **(A):** AlamarBlue assay to assess the cell growth of progerin-induced senescent mesenchymal stem cells (MSCs) incubated with induced pluripotent stem cell (iPSC)-EVs or MSC-EVs. **(B):** Results of the WST-1 assay for EV-treated MSCs. **(C):** Representative images of iPSC-EV- or MSC-EV-treated MSCs incubated with EdU. Scale bar: 100 μm. **(D):** Percentages of EdU positive cells after EV treatment of senescent MSCs. **(E):** Representative images of SA β-gal staining for senescent MSCs in the presence or absence of EVs. Scale bar: 50 μm. **(F):** Percentage of SA-β-gal-positive cells in senescent MSCs after EV treatment. **(G):** Real-time qPCR to detect *p21* and *p53* gene expression after iPSC-EV and MSC-EV treatment. Human GAPDH was used as the internal reference. All data reflect mean ± SD from three independent experiments. **, $p < .01$; ***, $p < .001$; $^{\#\#}$, $p < .01$; $^{\#\#\#}$, $p < .001$. Also see Supporting Information Figure S4.

Syndrome (HGPS), an early onset lethal premature aging disorder [33, 34]. As reported by previous studies using human fibroblasts and MSCs [35], the constitutive expression of progerin in MSCs resulted in senescence and other characteristic phenotypes of HGPS cells in culture (Supporting Information Fig. S4). However, when progerin-transduced MSCs were treated with highly purified EVs from iPSCs and MSCs, we observed enhanced cell growth as well as alleviation of aging cellular phenotypes (Fig. 4), as with the replicatively senescent MSCs shown in Figure 3.

EVs Produced by Human Stem Cells Contain a High Concentration of Intracellular Antioxidant Proteins Peroxiredoxins and Reduce Oxidative Stress in the Induced Senescent Cells

To investigate why EVs from human stem cells alleviate aging phenotypes of senescent cells, we analyzed the proteome of highly purified EVs from both types of stem cells as well as from human blood plasma. In total, we were able to detect 2,107 and 1,743 unique proteins in iPSC-EVs and MSC-EVs, respectively (Supporting Information Fig. S5A). We focused on the 1,135 unique proteins common to both types of EVs (Supporting Information Table S2). A gene ontology analysis showed that most of them are exosome- or lysosome-related proteins, such as CD9, CD63, and CD81 (Supporting Information Fig. S5B, Supporting Information Table S2). Among those 1,135 exosome-associated proteins, we noticed that several members of the peroxiredoxin (PRDX) family were highly abundant in iPSC-EVs and MSC-EVs, but much lower in plasma EVs (Fig. 5A; Supporting Information Fig. S5C). PRDXs, a class of antioxidant enzymes that are mainly located intracellularly with redox functions, have been reported to regulate longevity and stress resistance [36–38]. Because the PRDX1 and PRDX2 proteins have been reported to reduce cellular oxidative stress and senescence, which are often associated with aged or aging cells [39–42], we orthogonally verified the levels of these two antioxidant enzymes in purified EVs by Western blotting using specific antibodies (Fig. 5B). We confirmed that

A

Proteins	iPSC-EVs	MSC-EVs	Plasma-EVs
PRDX1	247790000	128490000	220390
PRDX6	74428000	99675000	0
PRDX2	63561000	29379000	370720
PRDX5	5910100	44411000	636840
PRDX4	4222600	4280700	0

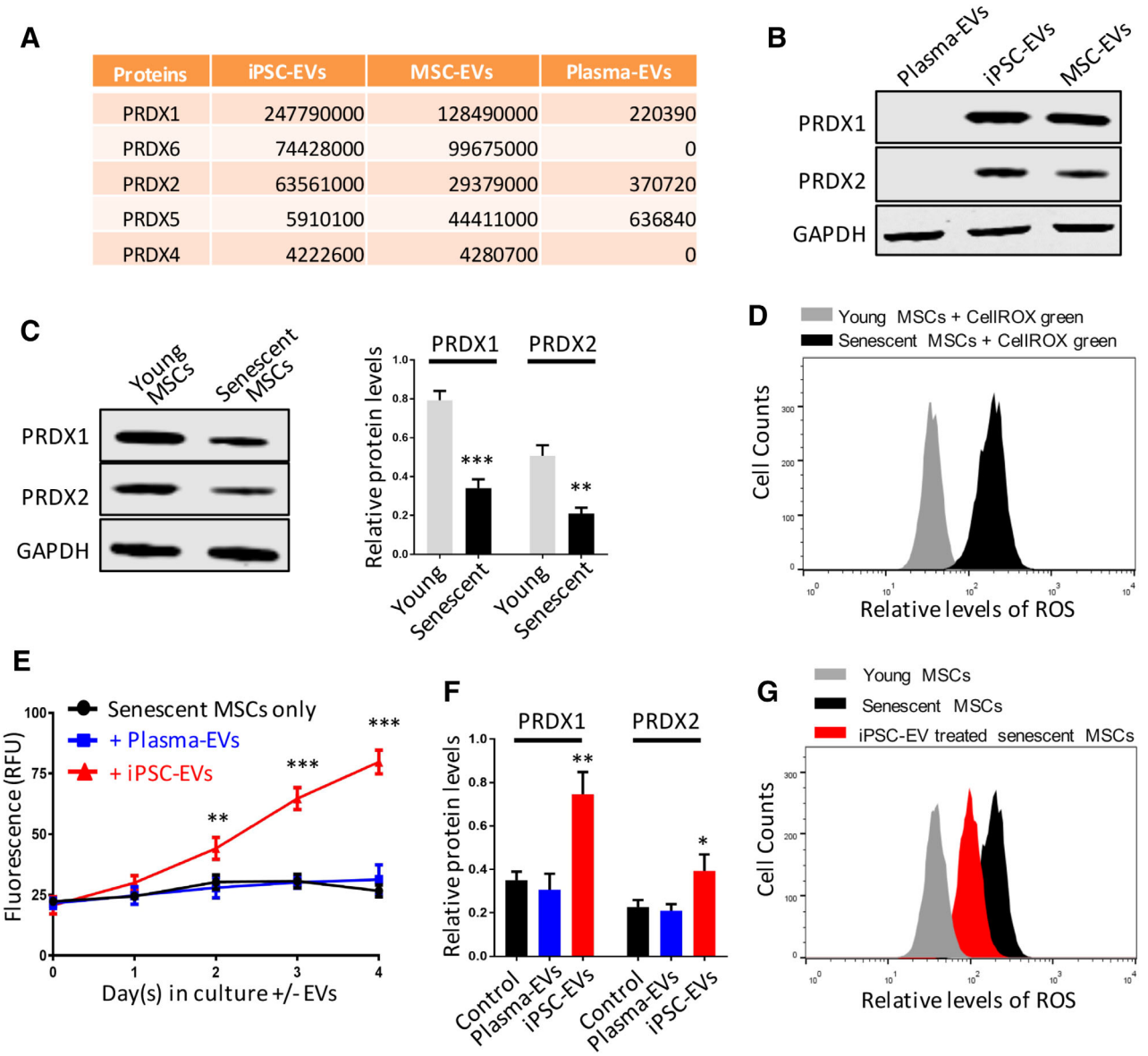

Figure 5. Stem cell-derived extracellular vesicles (EVs) contain high levels of peroxiredoxins and reduce cellular reactive oxygen species (ROS) in senescent cells. **(A):** Peroxiredoxin abundance in induced pluripotent stem cell (iPSC)-EVs and mesenchymal stem cell (MSC)-EVs by proteomics, rank by iBAQ intensities in iPSC-EVs. iBAQ, intensity based absolute quantification. **(B):** Western blotting to examine the protein level of PRDX1 and PRDX2 in plasma-EVs, iPSC-EVs and MSC-EVs. **(C):** Western blotting analysis of PRDX1 and PRDX2 proteins in young MSCs (passage 3) and senescent MSCs (progerin-induced). **(D):** Detection of cellular ROS by CellROX green in young MSCs (passage 3) and senescent MSCs (progerin-induced). **(E):** AlamarBlue fluorometric assay to assess the cell growth of progerin-induced senescent MSCs (control) compared with those treated with plasma-EVs or iPSC-EVs for 4 days. **(F):** Quantitation of PRDX1 and PRDX2 protein levels measured by Western blotting in cells cultured for 4 days with or without treatment with plasma-EVs or iPSC-EVs. **(G):** Detection of reduced cellular ROS level after treatment with iPSC-EVs (red) versus untreated senescent MSCs (black). All data reflect mean ± SD from four independent experiments. *, $p < .05$; **, $p < .01$; ***, $p < .001$. Also see Supporting Information Figure S5 and Supporting Information Table S2.

PRDX1 and PRDX2 are present in high levels in EVs derived from the two stem cell types but could not be detected in purified EVs from human plasma, consistent with the proteomic data (Fig. 5A). We also examined the levels of PRDX1 and PRDX2 proteins in young MSCs (passage 3) before and after progerin-mediated induction of senescence (Fig. 5C). The levels of PRDX1 and PRDX2 antioxidant proteins inversely correlated with the levels of cellular reactive oxygen species (ROS) measured with a previously established method [35]. Consistent with the previous observation [35], progerin-induced senescent MSCs showed a significantly higher level of cellular ROS compared with early-passage MSCs without progerin-induced senescence (Fig. 5D).

We next examined the cytoprotective or growth stimulatory effects of human iPSC-EVs and plasma-EVs on progerin-senescent MSCs. After treatment with the same numbers of EVs for 4 days (Fig. 5E), purified iPSC-EVs stimulated the growth of senescent MSCs as we observed before (Fig. 4A). However, the purified EVs from human blood plasma lacking PRDX1 and PRDX2 antioxidant proteins had little effect. Senescent MSCs treated with iPSC-EVs also showed elevated levels of PRDX1 and PRDX2 (Fig. 5F) and a

reduced level of cellular ROS (Fig. 5G). These data strongly suggest that PRDXs delivered by stem cell-derived EVs are responsible at least in part for the observed alleviation of oxidative stress and associated cellular aging.

Discussion

Until recently, most studies of EV-mediated tissue regeneration or repair used culture-expanded MSCs and showed medicinal benefits, at least transiently, after being introduced in vivo. Ongoing research efforts seek to achieve more efficient proliferation of cultured MSCs under chemically defined conditions and improved EV production. In this study, we compared production and function of EVs of human MSCs and iPSCs cultured under the same chemically defined culture condition. We showed that human iPSCs produced EVs >16-fold more efficiently than early-passage MSCs, from an aspect of producing high-concentrations of EVs released in medium by cultured cells. In addition, iPSC-EVs showed superior internalization by recipient cells and alleviation of aging phenotypes when applied to two aging models of human MSCs. The more abundant EV production from human iPSCs (that can be cultured infinitely using a chemically defined medium) also makes it more feasible for both laboratory research and future clinical applications that require a large number of purified EVs. Other methods such as anion exchange chromatography may help independently validate our EV purification scheme or further improve EV purification.

Recently, EVs produced from cultured MSCs were used to rejuvenate aged hematopoietic stem cells or MSCs [43, 44]. It was reported that young (p2–p6) MSCs produced EVs that could rejuvenate aged murine hematopoietic stem cells in a mouse model [43], similar to a previous report using MSC-EVs and an irradiation injury mouse model [10]. These studies have provoked great interest in examining the roles of EVs in cellular senescence and aging [45]. During the preparation of this article, Park et al. published a paper showing that human iPSC-EVs ameliorated aging of skin fibroblasts in vitro using an irradiation model [46]. Together, these studies firmly demonstrate that iPSC-EVs and MSC-EVs can alleviate senescence of human cells in vitro. However, early studies did not shed light on how EVs from human stem cells alleviate the aging phenotypes on senescent cells. Our current studies provide a new mechanism and strong evidence for the first time that stem cell-derived EVs carry a high level of PRDX antioxidant enzymes, which are at least in part responsible for the amelioration of aging phenotypes in progerin-induced senescent cells by reducing cellular ROS in these cells. Considering the many shared molecular and cellular mechanisms between premature aging and replicative senescence [34], we expect that PRDX antioxidant enzymes that can be delivered by EVs also play roles in replicative senescence and aging related diseases.

Although iPSC-derived EVs offer advantages in being produced in greater numbers and in stimulating cell metabolism, EVs from MSCs or other cell types that carry distinct cargos may be better suited for other medicinal applications. Recently, a proteomics study illustrated significant differences between human EVs produced by undifferentiated iPSCs and ones produced by iPSC-derived isogenic MSCs [47]. The former contains more cellular components of active cellular metabolism (consistent with our findings), whereas the latter acquires more stromal cell-associated modulatory activities [47]. One can envision that iPSC-derived EVs may be more efficient in medicinal applications to overcome cellular senescence, whereas EVs produced by various types of MSCs may be better suited to treat stromal disorders of collective tissues.

It remains to be determined if stem cell-derived EVs may also influence other pathways, such as the NRF2-mediated antioxidative regulation reported in a recent study using the same type of cellular model [35]. This regulation could occur in cooperation with or independent of intracellular PRDX antioxidant enzymes delivered by EVs. Despite our novel finding of EV-delivered PRDXs, it remains unclear whether additional bioactive molecules (proteins, RNAs, lipids, etc.) are involved in the alleviation of senescence. For example, mouse exosomal RNAs from hypothalamic stem/progenitor cells declined during aging, whereas treatment with healthy hypothalamic stem/progenitor cell-secreted exosomes led to the slowing of aging [48]. More studies are needed to extrapolate these findings to other species and other tissues.

Our defined in vitro cell culture systems using two aging models will likely help us elucidate shared mechanisms of aging and aging-associated diseases. The systems may also allow us to explore how stem cell derivatives can attenuate, ameliorate or reverse aging or disease phenotypes. As compared with potent human iPSCs, EVs that lack nuclei and cell proliferation potential offer an attractive, safer alternative for cellular therapy and regenerative medicine [17, 49]. A deeper understanding of how stem cell-derived EVs and their cargos alleviate aging phenotypes may help us achieve in vivo amelioration of aging-associated phenotypes, as reported recently in a small animal model [50].

Conclusion

We demonstrate that human iPSCs produce great numbers of EVs under a defined culture condition, and the concentration is 16-fold higher than by MSCs. Highly purified EVs secreted from both iPSCs and young MSCs alleviated senescence associated cellular phenotypes of aged MSCs through reducing intracellular ROS level via exosomal transfer of PRDXs. Our findings suggest that EVs from human stem cells offer an attractive, safer alternative for regenerative medicine and cellular therapy.

Acknowledgments

We thank Dr. Nicole Noren Hooten in NIA for suggestions for assays of cellular senescence phenotypes, Dr. David Clark, and Dr. Hui Zhang in Johns Hopkins' Mass Spectrometry Core Facility in the Center for Biomarker Discovery and Translation for proving expert proteomic analysis of purified EVs. This study was supported in part by grants from Maryland Stem Cell Research Fund (2016-MSCRFE-2739 and 2017-MSCRFD-3861) and National Institutes of Health (R56 AG-057430). L.C. is the Lucas and Lynn Chair of Hematology in the Johns Hopkins University.

Author Contributions

S.L.: conception and design, collection and/or assembly of data, data analysis and interpretation, manuscript writing; V.M.: conception and design, financial support, collection and/or assembly of data, manuscript writing; H.B.: conception and design, collection and/or assembly of data, manuscript writing; Z.D.: collection and/or assembly of data, data analysis and interpretation, provision of study material; J.L.: collection and/or assembly of data,

provision of study material. K.W.W.: manuscript writing, final approval of manuscript; L.C.: conception and design, financial support, administrative support, provision of study material, final approval of manuscript.

Disclosure of Potential Conflicts of Interest

On behalf of L.C., H.B., and V.M., Johns Hopkins University filed a patent application covering some aspects of human iPSC-derived EVs. Issues related to intellectual properties will be managed by Johns Hopkins Technology Ventures according to existing and standard policies. The other authors indicated no potential conflicts of interest.

Data Availability Statement

The data that support the findings of this study are available from the corresponding author upon reasonable request.

References

1 Colombo M, Raposo G, Thery C. Biogenesis, secretion, and intercellular interactions of exosomes and other extracellular vesicles. Annu Rev Cell Dev Biol 2014;30:255–289.

2 van Niel G, D'Angelo G, Raposo G. Shedding light on the cell biology of extracellular vesicles. Nat Rev Mol Cell Biol 2018;19:213–228.

3 Valadi H, Ekstrom K, Bossios A et al. Exosome-mediated transfer of mRNAs and microRNAs is a novel mechanism of genetic exchange between cells. Nat Cell Biol 2007;9:654–659.

4 Tkach M, Thery C. Communication by extracellular vesicles: Where we are and where we need to go. Cell 2016;164:1226–1232.

5 Hervera A, De Virgiliis F, Palmisano I et al. Reactive oxygen species regulate axonal regeneration through the release of exosomal NADPH oxidase 2 complexes into injured axons. Nat Cell Biol 2018;20:307–319.

6 ElAndaloussi S, Mager I, Breakefield XO et al. Extracellular vesicles: Biology and emerging therapeutic opportunities. Nat Rev Drug Discov 2013;12:347–357.

7 Lamichhane TN, Sokic S, Schardt JS et al. Emerging roles for extracellular vesicles in tissue engineering and regenerative medicine. Tissue Eng Part B Rev 2015;21:45–54.

8 Phinney DG, Pittenger MF. Concise review: MSC-derived exosomes for cell-free therapy. Stem Cells 2017;35:851–858.

9 Ibrahim AG, Cheng K, Marban E. Exosomes as critical agents of cardiac regeneration triggered by cell therapy. Stem Cell Rep 2014;2:606–619.

10 Wen S, Dooner M, Cheng Y et al. Mesenchymal stromal cell-derived extracellular vesicles rescue radiation damage to murine marrow hematopoietic cells. Leukemia 2016;30:2221–2231.

11 Furuta T, Miyaki S, Ishitobi H et al. Mesenchymal stem cell-derived exosomes promote fracture healing in a mouse model. Stem Cells Translational Medicine 2016;5:1620–1630.

12 de Godoy MA, Saraiva LM, de Carvalho LRP et al. Mesenchymal stem cells and cell-derived extracellular vesicles protect hippocampal neurons from oxidative stress and synapse damage induced by amyloid-beta oligomers. J Biol Chem 2018;293:1957–1975.

13 Bobis-Wozowicz S, Kmiotek K, Sekula M et al. Human induced pluripotent stem cell-derived microvesicles transmit RNAs and proteins to recipient mature heart cells modulating cell fate and behavior. Stem Cells 2015;33:2748–2761.

14 Bobis-Wozowicz S, Kmiotek K, Kania K et al. Diverse impact of xeno-free conditions on biological and regenerative properties of hUC-MSCs and their extracellular vesicles. J Mol Med 2017;95:205–220.

15 Chen G, Gulbranson DR, Hou Z et al. Chemically defined conditions for human iPSC derivation and culture. Nat Methods 2011;8:424–429.

16 Wang Y, Chou BK, Dowey S et al. Scalable expansion of human induced pluripotent stem cells in the defined xeno-free E8 medium under adherent and suspension culture conditions. Stem Cell Res 2013;11:1103–1116.

17 Nishiga M, Guo H, Wu JC. Induced pluripotent stem cells as a biopharmaceutical factory for extracellular vesicles. Eur Heart J 2018;39:1848–1850.

18 Saito S, Hiemori K, Kiyoi K et al. Glycome analysis of extracellular vesicles derived from human induced pluripotent stem cells using lectin microarray. Sci Rep 2018;8:3997.

19 Ding Q, Sun R, Wang P et al. Protective effects of human induced pluripotent stem cell-derived exosomes on high glucose-induced injury in human endothelial cells. Exp Ther Med 2018;15:4791–4797.

20 Zhang J, Guan J, Niu X et al. Exosomes released from human induced pluripotent stem cells-derived MSCs facilitate cutaneous wound healing by promoting collagen synthesis and angiogenesis. J Transl Med 2015;13:49.

21 Nong K, Wang W, Niu X et al. Hepatoprotective effect of exosomes from human-induced pluripotent stem cell-derived mesenchymal stromal cells against hepatic ischemia-reperfusion injury in rats. Cytotherapy 2016;18:1548–1559.

22 Qi X, Zhang J, Yuan H et al. Exosomes secreted by human-induced pluripotent stem cell-derived mesenchymal stem cells repair critical-sized bone defects through enhanced angiogenesis and osteogenesis in osteoporotic rats. Int J Biol Sci 2016;12:836–849.

23 Zhu Y, Wang Y, Zhao B et al. Comparison of exosomes secreted by induced pluripotent stem cell-derived mesenchymal stem cells and synovial membrane-derived mesenchymal stem cells for the treatment of osteoarthritis. Stem Cell Res Ther 2017;8:64.

24 Lotvall J, Hill AF, Hochberg F et al. Minimal experimental requirements for definition of extracellular vesicles and their functions: A position statement from the International Society for Extracellular Vesicles. J Extracellular Vesicles 2014;3:26913.

25 Witwer KW, Soekmadji C, Hill AF et al. Updating the MISEV minimal requirements for extracellular vesicle studies: Building bridges to reproducibility. J Extracellular Vesicles 2017;6:1396823.

26 Chou BK, Gu H, Gao Y et al. A facile method to establish human induced pluripotent stem cells from adult blood cells under feeder-free and xeno-free culture conditions: A clinically compliant approach. Stem Cells Translational Medicine 2015;4:320–332.

27 Chou BK, Mali P, Huang X et al. Efficient human iPS cell derivation by a non-integrating plasmid from blood cells with unique epigenetic and gene expression signatures. Cell Res 2011;21:518–529.

28 Mahairaki V, Ryu J, Peters A et al. Induced pluripotent stem cells from familial Alzheimer's disease patients differentiate into mature neurons with amyloidogenic properties. Stem Cells Dev 2014;23:2996–3010.

29 Cheng L, Hammond H, Ye Z et al. Human adult marrow cells support prolonged expansion of human embryonic stem cells in culture. Stem Cells 2003;20:121–132.

30 Cai J, Miao X, Li Y et al. Whole-genome sequencing identifies genetic variances in culture-expanded human mesenchymal stem cells. Stem Cell Rep 2014;3:227–233.

31 Noren Hooten N, Evans MK. Techniques to induce and quantify cellular senescence. J Vis Exp 2017;123:e55533.

32 Scaffidi P, Misteli T. Lamin A-dependent misregulation of adult stem cells associated with accelerated ageing. Nat Cell Biol 2008;10:452–459.

33 Gordon LB, Rothman FG, Lopez-Otin C et al. Progeria: A paradigm for translational medicine. Cell 2014;156:400–407.

34 Kubben N, Misteli T. Shared molecular and cellular mechanisms of premature ageing and ageing-associated diseases. Nat Rev Mol Cell Biol 2017;18:595–609.

35 Kubben N, Zhang W, Wang L et al. Repression of the antioxidant NRF2 pathway in premature aging. Cell 2016;165:1361–1374.

36 Detienne G, De Haes W, Mergan L et al. Beyond ROS clearance: Peroxiredoxins in stress signaling and aging. Ageing Res Rev 2018;44:33–48.

37 Rhee SG, Kil IS. Multiple functions and regulation of mammalian peroxiredoxins. Annu Rev Biochem 2017;86:749–775.

38 Radyuk SN, Orr WC. The multifaceted impact of peroxiredoxins on aging and disease. Antioxid Redox Signal 2018;29:1293–1311.

39 Park YH, Kim HS, Lee JH et al. Peroxiredoxin I participates in the protection of reactive oxygen species-mediated cellular senescence. BMB Rep 2017;50:528–533.

40 Aeby E, Ahmed W, Redon S et al. Peroxiredoxin 1 protects telomeres from oxidative damage and preserves telomeric DNA for extension by telomerase. Cell Rep 2016;17:3107–3114.

41 Han YH, Kim HS, Kim JM et al. Inhibitory role of peroxiredoxin II (Prx II) on cellular senescence. FEBS Lett 2005;579:4897–4902.

42 Han YH, Kwon JH, Yu DY et al. Inhibitory effect of peroxiredoxin II (Prx II) on Ras-ERK-NFkappaB pathway in mouse embryonic fibroblast (MEF) senescence. Free Radic Res 2006; 40:1182–1189.

43 Kulkarni R, Bajaj M, Ghode S et al. Intercellular transfer of microvesicles from young mesenchymal stromal cells rejuvenates aged murine hematopoietic stem cells. Stem Cells 2018;36:420–433.

44 Lei Q, Liu T, Gao F et al. Microvesicles as potential biomarkers for the identification of senescence in human mesenchymal stem cells. Theranostics 2017;7:2673–2689.

45 Takasugi M. Emerging roles of extracellular vesicles in cellular senescence and aging. Aging Cell 2018;17:e12734.

46 Oh M, Lee J, Kim YJ et al. Exosomes derived from human induced pluripotent stem cells ameliorate the aging of skin fibroblasts. Int J Mol Sci 2018;19(6):1715.

47 La Greca A, Solari C, Furmento V et al. Extracellular vesicles from pluripotent stem cell-derived mesenchymal stem cells acquire a stromal modulatory proteomic pattern during differentiation. Exp Mol Med 2018;50:119.

48 Zhang Y, Kim MS, Jia B et al. Hypothalamic stem cells control ageing speed partly through exosomal miRNAs. Nature 2017;548:52–57.

49 Adamiak M, Cheng G, Bobis-Wozowicz S et al. Induced pluripotent stem cell (iPSC)-derived extracellular vesicles are safer and more effective for cardiac repair than iPSCs. Circ Res 2018;122:296–309.

50 Ocampo A, Reddy P, Martinez-Redondo P et al. In vivo amelioration of age-associated hallmarks by partial reprogramming. Cell 2016; 167:1719–1733.

See www.StemCells.com for supporting information available online.